Available online at www.sciencedirect.com
ScienceDirect
Journal of Sound and Vibration 307 (2007) 250–264
JOURNAL OF SOUND AND VIBRATION
www.elsevier.com/locate/jsvi

Dynamic stability of a non-conservative viscoelastic rectangular plate

Zhong-Min Wang, Yin-Feng Zhou*, Yan Wang

School of Sciences, Xi'an University of Technology, 710048 Xi'an, China

Received 26 January 2007; received in revised form 18 April 2007; accepted 1 July 2007

Abstract

Based on the thin-plate theory and the two-dimensional (2D) viscoelastic differential constitutive relation, the differential equation of motion of the viscoelastic rectangular plate subjected to uniformly distributed tangential follower force in Laplace domain is deduced, the equation is suitable for various viscoelastic models of differential type. The differential equation of motion of the viscoelastic plate constituted by the Kelvin–Voigt model under the action of uniformly distributed tangential follower force in time domain is also derived. The generalized eigenequations of non-conservative viscoelastic rectangular plate, with four edges simply supported, two opposite edges simply supported and other two edges clamped are established by the differential quadrature method, and the curves of real parts and imaginary parts of the first three-order dimensionless complex frequencies vs. uniformly distributed tangential follower force are obtained, the factors influencing the dynamic stability of the visoelastic rectangular plate are discussed.

1. Introduction

There exists a considerable literature devoted to the stability and vibration of the elastic plate subjected to non-conservative forces (in particular the follower forces). Adali [1] studied the stability of a plate under a follower force and an in-plane force. He showed that, depending on the relative magnitudes of the follower force and the in-plane force, the plate may lose its stability by flutter or divergence. Leipholz and Pfendt [2] used extended Galerkin's theory to analyze the plate with distributed follower forces acting on the surface of a plate. By the Levy method and the finite difference method, Wang and Ji [3] investigated the dynamic stability of six typical rectangular plates with two opposite edges simply supported under the action of a uniformly distributed tangential follower force. Zuo and Shreyer [4] described divergence and flutter instability regions for simply supported plates with a combination of fixed and follower forces. Kim and Park [5] investigated the dynamic stability of a completely free plate subjected to intermediate follower force. Kim and Kim [6] studied the dynamic stability of a plate under a follower force through the finite element method based on the Kirchhoff–Love plate theory and the Mindlin plate theory. Jayaraman

*Corresponding author.
E-mail address: yinfengzhou@163.com (Y.-F. Zhou).

0022-460X/$ - see front matter © 2007 Elsevier Ltd. All rights reserved.
doi:10.1016/j.jsv.2007.07.003

and Struthers [7] analyzed the divergence and flutter instabilities of an orthotropic rectangular plate subjected to follower forces.

With the wide application of viscoelastic materials nowadays, it is necessary to illustrate the viscoelastic properties of the structure. To the author's knowledge, there are relatively few investigations on the stability characteristics of the viscoelastic structure under follower force [8–10], however, most of these studies have been confined to unidimension, that is to say the research objects are the viscoelastic column and the viscoelastic beam. Few papers have been presented on stability problems for the non-conservative viscoelastic plate, because there are two difficulties in studying this problem, one is the complexity of the two-dimensional (2D) viscoelastic differential constitutive relation and the other is that the differential equation of motion of a non-conservative viscoelastic plate is a four-order partial differential equation with complex variable coefficient, which belongs to the complex eigenvalue problem.

The purposes of this paper are to establish the general differential equation of motion of a viscoelastic plate subjected to distributed tangential follower forces in time domain, to analyze the vibration and stability of a viscoelastic plate constituted by the Kelvin–Voigt model under the action of uniformly distributed tangential follower force and to study the effects of aspect ratio and dimensionless delay time on the dynamic stability of the viscoelastic plate constituted by the Kelvin–Voigt model.

2. Differential equation of a motion of non-conservative viscoelastic plate

Consider a viscoelastic rectangular thin plate subjected to uniformly distributed tangential follower force q_0, as shown in Fig. 1. The plate has the length a, width b and thickness h in the x, y and z direction, respectively, the density of the material is ρ.

The general 3D viscoelastic differential constitutive relation is as follows:

$$\begin{cases} P's_{ij} = Q'e_{ij}, \\ P''\sigma_{ii} = Q''\varepsilon_{ii}. \end{cases} \tag{1}$$

The Laplace transformation of Eq. (1)

$$\begin{cases} \bar{P}'\bar{s}_{ij} = \bar{Q}'\bar{e}_{ij}, \\ \bar{P}''\bar{\sigma}_{ii} = \bar{Q}''\bar{\varepsilon}_{ii}, \end{cases} \tag{2}$$

where s_{ij} and e_{ij} are deviatoric tensor of stress and strain, σ_{ii} and ε_{ii} are spherical tensor of stress and strain, and the operators

$$P' = \sum_{k=0}^{l} p'_k \frac{\mathrm{d}^k}{\mathrm{d}t^k}, \quad Q' = \sum_{k=0}^{r} q'_k \frac{\mathrm{d}^k}{\mathrm{d}t^k}, \quad P'' = \sum_{k=0}^{l_1} p''_k \frac{\mathrm{d}^k}{\mathrm{d}t^k}, \quad Q'' = \sum_{k=0}^{r_1} q''_k \frac{\mathrm{d}^k}{\mathrm{d}t^k}, \; p'_k,\; q'_k,\; p''_k,\; q''_k$$

depend on the properties of the material, and the bar on every operator and every function denotes the Laplace transformation.

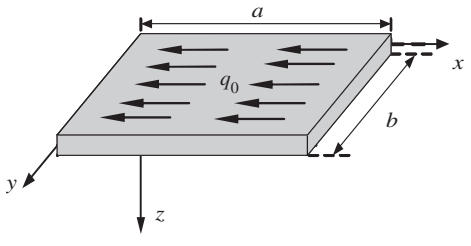

Fig. 1. Non-conservative viscoelastic rectangular plate.

For plane stress problem, the constitutive equations of the linear viscoelastic material in the Laplace domain [11] are

$$\begin{cases} \bar{P}'(\bar{P}'\bar{Q}'' + 2\bar{Q}'\bar{P}'')\bar{\sigma}_x = \bar{Q}'(2\bar{P}'\bar{Q}'' + \bar{Q}'\bar{P}'')\bar{\varepsilon}_x + \bar{Q}'(\bar{P}'\bar{Q}^{''} - \bar{Q}'\bar{P}'')\bar{\varepsilon}_y, \\ \bar{P}'(\bar{P}'\bar{Q}'' + 2\bar{Q}'\bar{P}'')\bar{\sigma}_y = \bar{Q}'(\bar{P}'\bar{Q}^{''} - \bar{Q}'\bar{P}'')\bar{\varepsilon}_x + \bar{Q}'(2\bar{P}'\bar{Q}'' + \bar{Q}'\bar{P}'')\bar{\varepsilon}_y, \\ \bar{P}'\bar{\tau}_{xy} = \bar{Q}'\bar{\varepsilon}_{xy}, \end{cases} \tag{3}$$

where $\bar{\sigma}_x$, $\bar{\sigma}_y$, $\bar{\tau}_{xy}$, $\bar{\varepsilon}_x$, $\bar{\varepsilon}_y$, $\bar{\varepsilon}_{xy}$ are the Laplace transforms of σ_x, σ_y, τ_{xy}, ε_x, ε_y, ε_{xy}, respectively, $\bar{P}^{'}$, $\bar{Q}^{'}$, $\bar{P}''$, $\bar{Q}''$ are the Laplace transforms of differential operators P', Q', P'', Q'', respectively.

Introducing the differential operators

$$\begin{cases} \bar{P}_0 = \bar{P}'(\bar{P}'\bar{Q}'' + 2\bar{Q}'\bar{P}''), \\ \bar{Q}_0 = \bar{Q}'(2\bar{P}'\bar{Q}'' + \bar{Q}'\bar{P}''), \\ \bar{Q}_1 = \bar{Q}'(\bar{P}'\bar{Q}^{''} - \bar{Q}'\bar{P}''). \end{cases} \tag{4}$$

Eq. (3) can be simplified as

$$\begin{cases} \bar{P}_0\bar{\sigma}_x = \bar{Q}_0\bar{\varepsilon}_x + \bar{Q}_1\bar{\varepsilon}_y, \\ \bar{P}_0\bar{\sigma}_y = \bar{Q}_1\bar{\varepsilon}_x + \bar{Q}_0\bar{\varepsilon}_y, \\ \bar{P}'\bar{\tau}_{xy} = \bar{Q}'\bar{\varepsilon}_{xy}. \end{cases} \tag{5}$$

The bending moment M_x, M_y, twisting moment M_{xy}, M_{yx} on the per unit length of the plate are

$$M_x = \int_{-h/2}^{h/2} z\sigma_x \,\mathrm{d}z, \quad M_y = \int_{-h/2}^{h/2} z\sigma_y \,\mathrm{d}z, \tag{6.1}$$

$$M_{xy} = \int_{-h/2}^{h/2} z\tau_{xy} \,\mathrm{d}z, \quad M_{yx} = \int_{-h/2}^{h/2} z\tau_{yx} \,\mathrm{d}z. \tag{6.2}$$

Applying the operators $\bar{P}_0$, $\bar{P}'$ to the Laplace transformation results of Eqs. (6.1) and (6.2), respectively, then

$$\begin{cases} \bar{P}_0(\bar{M}_x) = \int_{-h/2}^{h/2} z\bar{P}_0(\bar{\sigma}_x)\,\mathrm{d}z, \\ \bar{P}_0(\bar{M}_y) = \int_{-h/2}^{h/2} z\bar{P}_0(\bar{\sigma}_y)\,\mathrm{d}z, \\ \bar{P}'(\bar{M}_{xy}) = \int_{-h/2}^{h/2} z\bar{P}'(\bar{\tau}_{xy})\,\mathrm{d}z. \end{cases} \tag{7}$$

Substituting Eq. (5) into Eq. (7), one obtains the relations between moment and the Laplace transformation of deflection w as

$$\begin{cases} \bar{P}_0(\bar{M}_x) = -\int_{-h/2}^{h/2} z^2 \left[\bar{Q}_0\dfrac{\partial^2\bar{w}}{\partial x^2} + \bar{Q}_1\dfrac{\partial^2\bar{w}}{\partial y^2}\right]\mathrm{d}z, \\ \bar{P}_0(\bar{M}_y) = -\int_{-h/2}^{h/2} z^2 \left[\bar{Q}_1\dfrac{\partial^2\bar{w}}{\partial x^2} + \bar{Q}_0\dfrac{\partial^2\bar{w}}{\partial y^2}\right]\mathrm{d}z, \\ \bar{P}'(\bar{M}_{xy}) = \bar{P}'(\bar{M}_{yx}) = -\int_{-h/2}^{h/2} z\bar{Q}'\left(\dfrac{\partial^2\bar{w}}{\partial x\partial y}\right)\mathrm{d}z. \end{cases} \tag{8}$$

According to the D'Alembert principle, the equilibrium equation of the non-conservative plate can be given as

$$\frac{\partial^2 M_x}{\partial x^2} + 2\frac{\partial^2 M_{xy}}{\partial x\partial y} + \frac{\partial^2 M_y}{\partial y^2} - q_0(a-x)\frac{\partial^2 w}{\partial x^2} - \rho h\frac{\partial^2 w}{\partial t^2} = 0. \tag{9}$$

Applying $\bar{P}_0\bar{P}'$ to the Laplace transformation of Eq. (9), then

$$\bar{P}_0\bar{P}'\left(\frac{\partial^2\bar{M}_x}{\partial x^2}\right)+2\bar{P}_0\bar{P}'\left(\frac{\partial^2\bar{M}_{xy}}{\partial x\partial y}\right)+\bar{P}_0\bar{P}'\left(\frac{\partial^2\bar{M}_y}{\partial y^2}\right)-\bar{P}_0\bar{P}'q_0(a-x)\frac{\partial^2\bar{w}}{\partial x^2}-\rho h\bar{P}_0\bar{P}'s_1^2\bar{w}=0. \tag{10}$$

If the partial derivative is continuous, Eq. (10) can be rewritten as

$$\bar{P}'\left(\frac{\partial^2[\bar{P}_0(\bar{M}_x)]}{\partial x^2}\right)+2\bar{P}_0\left(\frac{\partial^2[\bar{P}'(\bar{M}_{xy})]}{\partial x\partial y}\right)+\bar{P}'\left(\frac{\partial^2[\bar{P}(\bar{M}_y)]}{\partial y^2}\right)-\bar{P}_0\bar{P}'q_0(a-x)\frac{\partial^2\bar{w}}{\partial x^2}-\rho h\bar{P}_0\bar{P}'s_1^2\bar{w}=0. \tag{11}$$

Substituting Eq. (7) into Eq. (11), the differential equation of the non-conservative viscoelastic plate in the Laplace domain is deduced as

$$\frac{h^3}{12}\bar{P}'\bar{Q}_0\nabla^4\bar{w}+\bar{P}_0\bar{P}'q_0(a-x)\frac{\partial^2\bar{w}}{\partial x^2}+\rho h\bar{P}_0\bar{P}'s_1^2\bar{w}=0. \tag{12}$$

Eq. (12) has extensive application and is suitable for various viscoelastic models, the corresponding differential equations can be obtained by substituting the different differential operters $\bar{P}_0$, $\bar{Q}_0$, $\bar{P}'$ into the equation.

Assuming that the material of the plate obeys elastic behavior in dilatation and the Kelvin–Voigt law in distortion, the constitutive equations are as follows [12]:

$$\begin{cases} s_{ij}=2Ge_{ij}+2\eta\dot{e}_{ij}, \\ \sigma_{ii}=3K\varepsilon_{ii}. \end{cases} \tag{13}$$

Performing the Laplace transformation on Eq. (13), we have

$$\begin{cases} \bar{P}'=1, \quad \bar{Q}'=2G+2\eta s_1, \\ \bar{P}''=1, \quad \bar{Q}''=3K. \end{cases} \tag{14}$$

Substituting Eq. (14) into Eq. (12), and carrying out the Laplace inverse transformation, a differential equation of the non-conservative viscoelastic rectangular plate constituted by the Kelvin–Voigt model in the time domain is obtained:

$$\frac{h^3}{12}\left(A_3+A_4\frac{\partial}{\partial t}+A_5\frac{\partial^2}{\partial t^2}\right)\nabla^4 w+q_0(a-x)\left(A_1+A_2\frac{\partial}{\partial t}\right)\frac{\partial^2 w}{\partial x^2}+\rho h\left(A_1+A_2\frac{\partial}{\partial t}\right)\frac{\partial^2 w}{\partial t^2}=0, \tag{15}$$

where $A_1=3K+4G$, $A_2=4\eta$, $A_3=2G(6K+2G)$, $A_4=8G\eta+12K\eta$, $A_5=4\eta^2$, $G=E/2(1+\mu)$, $K=E/3(1-2\mu)$, μ is Poisson's ratio,

$$\nabla^2 w=\frac{\partial^2 w}{\partial x^2}+\frac{\partial^2 w}{\partial y^2}, \quad \nabla^4 w=\frac{\partial^4 w}{\partial x^4}+2\frac{\partial^4 w}{\partial x^2\partial y^2}+\frac{\partial^4 w}{\partial y^4}.$$

Introduce the dimensionless variables and parameters

$$\begin{aligned} &\xi=\frac{x}{a}, \quad \psi=\frac{y}{b}, \quad \bar{W}=\frac{w}{h}, \quad \lambda=\frac{a}{b}, \quad q=\frac{12q_0a^3(1-\mu^2)}{Eh^3}, \\ &\tau=\frac{th}{a^2}\sqrt{\frac{E}{12\rho(1-\mu^2)}}, \quad H=\frac{h}{a^2}\sqrt{\frac{E}{12\rho(1-\mu^2)}}\,\frac{\eta}{E}. \end{aligned} \tag{16}$$

Eq. (15) can be rewritten as

$$\begin{aligned} &\left[1+\frac{4(2-\mu)(1+\mu)}{3}H\frac{\partial}{\partial\tau}+\frac{4(1-2\mu)(1+\mu)^2}{3}H^2\frac{\partial^2}{\partial\tau^2}\right]\nabla^4\bar{W} \\ &\quad+q(1-\xi)\left[1+\frac{4(1-2\mu)(1+\mu)}{3(1-\mu)}H\frac{\partial}{\partial\tau}\right]\frac{\partial^2\bar{W}}{\partial\xi^2}+\left[1+\frac{4(1-2\mu)(1+\mu)}{3(1-\mu)}H\frac{\partial}{\partial\tau}\right]\frac{\partial^2\bar{W}}{\partial\tau^2}=0, \end{aligned} \tag{17}$$

where τ is dimensionless time, H is the dimensionless delay time of the material and

$$\nabla^4 \bar{W} = \frac{\partial^4 \bar{W}}{\partial \xi^4} + 2\lambda^2 \frac{\partial^4 \bar{W}}{\partial \xi^2 \partial \psi^2} + \lambda^4 \frac{\partial^4 \bar{W}}{\partial \psi^4}.$$

Suppose that the solution to Eq. (17) takes the form

$$\bar{W}(\xi, \psi, \tau) = W(\xi, \psi)\, \mathrm{e}^{\mathrm{j}\omega\tau}, \tag{18}$$

where $\mathrm{j} = \sqrt{-1}$ and ω is the dimensionless complex frequency.

Substituting Eq. (18) into Eq. (17) gives

$$D_1 \nabla^4 W + q(1-\xi) D_2 \frac{\partial^2 W}{\partial \xi^2} + D_2 \mathrm{j}^2 \omega^2 W = 0, \tag{19}$$

where

$$D_1 = 1 + \frac{4(2-\mu)(1+\mu)}{3} H\omega\mathrm{j} - \frac{4(1-2\mu)(1+\mu)^2}{3} H^2\omega^2, \quad D_2 = 1 + \frac{4(1-2\mu)(1+\mu)}{3(1-\mu)} H\omega\mathrm{j},$$

$$\nabla^4 W = \frac{\partial^4 W}{\partial \xi^4} + 2\lambda^2 \frac{\partial^4 W}{\partial \xi^2 \partial \psi^2} + \lambda^4 \frac{\partial^4 W}{\partial \psi^4}.$$

The boundary conditions of the plate with four edges simply supported are as follows:

$$\begin{cases} \xi = 0, 1: & W(\xi, \psi) = \dfrac{\partial^2 W}{\partial \xi^2} = 0, \\ \psi = 0, 1: & W(\xi, \psi) = \dfrac{\partial^2 W}{\partial \psi^2} = 0. \end{cases} \tag{20}$$

The boundary conditions of the plate with two opposite edges simply supported and other two edges clamped are as follows:

$$\begin{cases} \xi = 0, 1: & W(\xi, \psi) = \dfrac{\partial W}{\partial \xi} = 0, \\ \psi = 0, 1: & W(\xi, \psi) = \dfrac{\partial^2 W}{\partial \psi^2} = 0. \end{cases} \tag{21}$$

3. Differential quadrature (DQ) method

The basic idea of the DQ method [13] is to approximate the partial derivatives of a function with respect to a spatial variable at any discrete point as the weighted linear sum of the function values at all the discrete points chosen in the solution domain of the spatial variable. Postulating smooth function $f(x, y)$ in region $0 \leqslant x \leqslant a$, $0 \leqslant y \leqslant b$, the rth order partial derivative of $f(x, y)$ with respect to x, the sth order partial derivative of $f(x, y)$ with respect to y and the $(r+s)$th order mixed partial derivative of $f(x, y)$ with respect to both x and y can be discretely expressed at the point (x_i, y_j) as [14]

$$\frac{\partial^r f(x_i, y_j)}{\partial x^r} = \sum_{k=1}^{N} A_{ik}^{(r)} f(x_k, y_j) \quad (i = 1, 2, \ldots, N;\ r = 1, 2, \ldots, N-1), \tag{22}$$

$$\frac{\partial^s f(x_i, y_j)}{\partial y^s} = \sum_{m=1}^{M} A_{jm}^{(s)} f(x_i, y_m) \quad (j = 1, 2, \ldots, M;\ s = 1, 2, \ldots, M-1), \tag{23}$$

$$\frac{\partial^{r+s} f(x_i, y_j)}{\partial x^r \partial y^s} = \sum_{k=1}^{N} A_{ik}^{(r)} \sum_{m=1}^{M} A_{jm}^{(s)} f(x_i, y_m), \tag{24}$$

where N, M is the number of grid points in the x and y direction, respectively, $A_{ik}^{(r)}$ and $A_{jm}^{(s)}$ are the weighted coefficients, and they are defined by [15]

$$A_{ik}^{(1)} = \begin{cases} \prod\limits_{\substack{\mu=1 \\ \mu \neq i,k}}^{N} (x_i - x_\mu) \Big/ \prod\limits_{\substack{\mu=1 \\ \mu \neq k}}^{N} (x_k - x_\mu) & (i,k = 1,2,\ldots,N;\ k \neq i), \\ \sum\limits_{\substack{\mu=1 \\ \mu \neq i}}^{N} \dfrac{1}{x_i - x_\mu} & (i,k = 1,2,\ldots,N;\ k = i), \end{cases} \tag{25}$$

$$A_{jm}^{(1)} = \begin{cases} \prod\limits_{\substack{\mu=1 \\ \mu \neq j,m}}^{M} (y_j - y_\mu) \Big/ \prod\limits_{\substack{\mu=1 \\ \mu \neq m}}^{M} (y_m - y_\mu) & (j,m = 1,2,\ldots,M;\ m \neq j), \\ \sum\limits_{\substack{\mu=1 \\ \mu \neq j}}^{M} \dfrac{1}{y_j - y_\mu} & (j,m = 1,2,\ldots,M;\ m = j). \end{cases} \tag{26}$$

In the case of $r = 2,3,\ldots,N-1;\ s = 2,3,\ldots,M-1$,

$$A_{ik}^{(r)} = \begin{cases} r\left(A_{ii}^{(r-1)} A_{ik}^{(1)} - \dfrac{A_{ik}^{(r-1)}}{x_i - x_k}\right) & (i,k = 1,2,\ldots,N;\ k \neq i), \\ -\sum\limits_{\substack{\mu=1 \\ \mu \neq i}}^{N} A_{i\mu}^{(r)} & (i = 1,2,\ldots,N;\ 1 \leqslant r \leqslant (N-1)), \end{cases} \tag{27}$$

$$A_{jm}^{(s)} = \begin{cases} s\left(A_{jj}^{(s-1)} A_{jm}^{(1)} - \dfrac{A_{jm}^{(s-1)}}{y_j - y_m}\right) & (j,m = 1,2,\ldots,M;\ m \neq j), \\ -\sum\limits_{\substack{\mu=1 \\ \mu \neq j}}^{M} A_{j\mu}^{(s)} & (j = 1,2,\ldots,M;\ \ 1 \leqslant s \leqslant (M-1)). \end{cases} \tag{28}$$

In this paper, the distribution forms of the grid points are non-uniform, the plate with four edges simply supported adopts the weighted coefficient method to treat the boundary conditions and the plate with two opposite edges simply supported and other edges clamped adopts the δ method combining with the weighted coefficient method to treat the boundary conditions. The distribution forms of the grid points are

$$\begin{cases} \xi_1 = 0, \quad \xi_N = 1, \quad \xi_i = \dfrac{1}{2}\left[1 - \cos\left(\dfrac{2i-3}{2N-4}\pi\right)\right] & (i = 2,3\cdots N-1), \\ \psi_1 = 0, \quad \psi_N = 1, \quad \psi_i = \dfrac{1}{2}\left[1 - \cos\left(\dfrac{2i-3}{2N-4}\pi\right)\right] & (i = 2,3\cdots N-1), \end{cases} \tag{29}$$

$$\begin{cases} \xi_1 = 0, \quad \xi_2 = \delta, \quad \xi_{N-1} = 1-\delta, \quad \xi_N = 1, \quad \xi_i = \dfrac{1}{2}\left[1 - \cos\left(\dfrac{i-2}{N-3}\pi\right)\right] & (i = 3,4,\ldots,N-2), \\ \psi_1 = 0, \quad \psi_N = 1, \quad \psi_i = \dfrac{1}{2}\left[1 - \cos\left(\dfrac{2i-3}{2N-4}\pi\right)\right] & (i = 2,3,\ldots,N-1). \end{cases} \tag{30}$$

According to the DQ method's procedures, Eq. (19) can be *discretized* into the following forms:

$$\left(\sum_{k=1}^{N} A_{ik}^{(4)} W_{kj} + 2\lambda^2 \sum_{m=1}^{N} A_{jm}^{(2)} \sum_{k=1}^{N} A_{ik}^{(2)} W_{km} + \lambda^4 \sum_{k=1}^{N} A_{jk}^{(4)} W_{ik}\right) + q(1-\xi) \sum_{k=1}^{N} A_{ik}^{(2)} W_{kj}$$
$$+ \left[\frac{4(2-\mu)(1+\mu)}{3} H\mathrm{j}\left(\sum_{k=1}^{N} A_{ik}^{(4)} W_{kj} + 2\lambda^2 \sum_{m=1}^{N} A_{jm}^{(2)} \sum_{k=1}^{N} A_{ik}^{(2)} W_{km} + \lambda^4 \sum_{k=1}^{N} A_{jk}^{(4)} W_{ik}\right)\right.$$
$$\left. + \frac{4(1-2\mu)(1+\mu)}{3(1-\mu)} H\mathrm{j} q(1-\xi) \sum_{k=1}^{N} A_{ik}^{(2)} W_{kj}\right] \omega + \frac{4(1-2\mu)(1+\mu)}{3(1-\mu)} H^3 \mathrm{j}^3 W \omega^3$$
$$+ \left[\frac{4(1-2\mu)(1+\mu)^2}{3} H^2 j^2 \left(\sum_{k=1}^{N} A_{ik}^{(4)} W_{kj} + 2\lambda^2 \sum_{m=1}^{N} A_{jm}^{(2)} \sum_{k=1}^{N} A_{ik}^{(2)} W_{km} + \lambda^4 \sum_{k=1}^{N} A_{jk}^{(4)} W_{ik}\right) + \mathrm{j}^2 W\right] \omega^2 = 0. \tag{31}$$

The differential quadrature form of boundary conditions (20) are

$$\begin{cases} W_{1j} = W_{Nj} = W_{i1} = W_{iN} = 0, & i,j = 1,2,\ldots,N, \\ \sum\limits_{k=1}^{N} A_{ik}^{(2)} W_{kj} = 0, & i = 1,N, \quad j = 1,2,\ldots,N, \\ \sum\limits_{k=1}^{N} A_{jk}^{(2)} W_{ik} = 0, & j = 1,N, \quad i = 1,2,\ldots,N \end{cases} \tag{32}$$

the differential quadrature form of boundary conditions (21) are

$$\begin{cases} W_{1j} = W_{Nj} = W_{i1} = W_{iN} = 0, & i,j = 1,2,\ldots,N, \\ \sum\limits_{k=1}^{N} A_{ik}^{(1)} W_{kj} = 0, & i = 2,N-1, \quad j = 2,3,\ldots,N-2, \\ \sum\limits_{k=1}^{N} A_{jk}^{(2)} W_{ik} = 0, & j = 1,N, \quad i = 1,2,\ldots,N. \end{cases} \tag{33}$$

Eq. (31) and boundary conditions (32) or (33) can be written in the matrix form as

$$\left(\omega^3[Q] + \omega^2[R] + \omega[G] + [K]\right)\{W_{kj}\} = \{0\}, \tag{34}$$

where the matrices $[Q]$, $[R]$, $[G]$ and $[K]$ involve such parameters as dimensionless delay time H, dimensionless follower force and aspect ratio of the plate. Eq. (34) is a generalized eigenvalue problem.

4. Results and discussions

In the case of $H = 0$, Eq. (19) is reduced to the differential equation of motion of the non-conservative elastic plate. In order to verify the DQ method, the first three-order natural frequencies and the critical loads of the non-conservative elastic plate with two different boundary conditions are calculated firstly. The results in this paper are in good agreement with those in Refs. [16,3], which can be seen from Tables 1 and 2. The node number $N = 9$.

In Table 2, q_{d1} and q_{d2} denote the first and the second-order divergence load, respectively, q_f denotes the flutter load. Now, the dynamic stability of the non-conservative viscoelastic rectangular plate constituted by the Kelvin–Voigt model is calculated and analyzed.

4.1. The plate with four edges simply supported

Fig. 2 shows the variation of the first three-order dimensionless complex frequencies of the viscoelastic plate with dimensionless follower force q for $H = 10^{-5}$, $\lambda = 1$. It can be seen that when dimensionless follower force

Table 1
Comparison of the first three natural frequencies of elastic plate with reference [16]

Aspect ratio, λ	Boundary condition	The solution in this paper			Exact solution [16]		
1	SSSS	19.73	49.35	78.98	19.73	49.35	78.98
	CSCS	28.95	54.74	69.33	28.95	54.74	69.33
1.5	SSSS	32.07	61.68	98.70	32.07	61.68	98.69
	CSCS	39.09	79.53	102.22	39.08	79.52	102.21
2	SSSS	49.34	78.96	127.56	49.34	78.96	128.30
	CSCS	54.74	94.59	154.87	54.76	94.60	154.76

Table 2
Comparison of the critical load of elastic plate with Ref. [3]

Aspect ratio, λ	Boundary condition	The solution in this paper	Existing results [3]
1	SSSS	$q_{d1} = 67.5$, $q_{d2} = 132.10$	$q_{d1} = 67.4$, $q_{d2} = 131.60$
	CSCS	$q_{d1} = 143.5$, $q_f = 168$	–
1.5	SSSS	$q_{d1} = 136.75$, $q_{d2} = 224.72$	$q_{d1} = 136.56$, $q_{d2} = 221.28$
	CSCS	$q_f = 202.75$	–
2	SSSS	$q_{d1} = 224.8$, $q_{d2} = 340.5$	$q_{d1} = 223.55$, $q_{d2} = 340.34$
	CSCS	$q_f = 251.5$	–

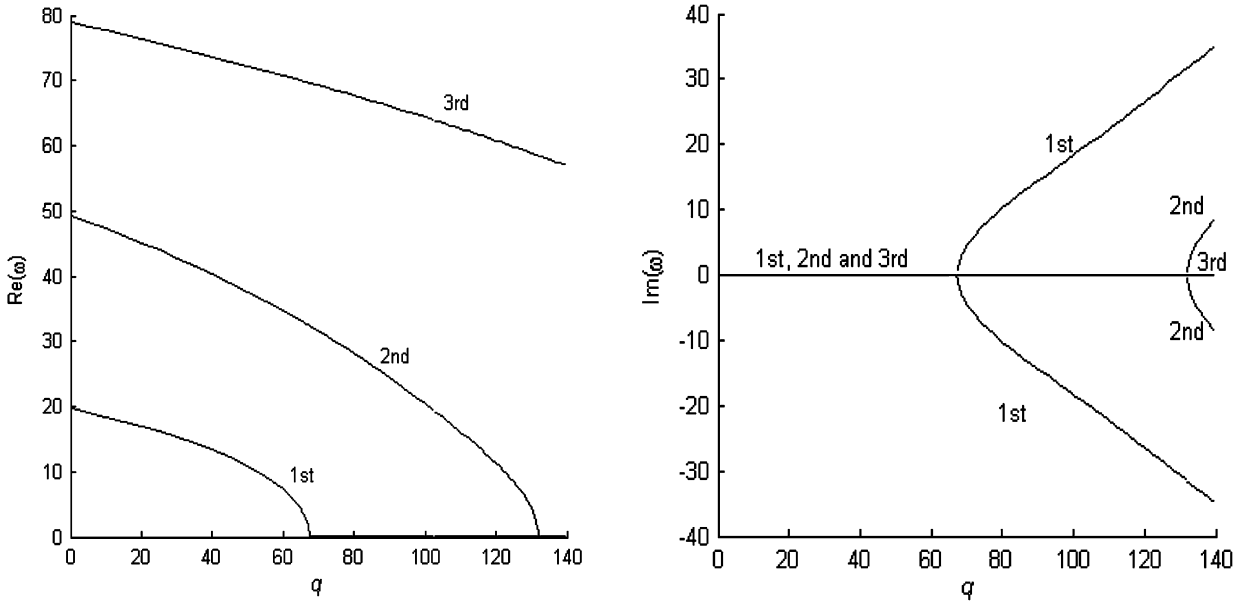

Fig. 2. The first three dimensionless complex frequencies ω vs. dimensionless follower force q for SSSS plate for $H = 10^{-5}$, $\lambda = 1$.

$q = 0$, the first three-order natural frequencies of the viscoelastic plate in Fig. 2 are exactly the same as those in Ref. [16]. With increase of q, the real part of ω decreases, while its imaginary part remains zero. With the further increase of q, the real parts of ω in the first and the second mode successively become zero, and then the imaginary parts of ω have two branches with positive and negative values. This shows that the viscoelastic plate shows divergence instability. The first and the second order divergence load is $q_{d1} = 67.5$ and $q_{d2} = 132.10$, respectively.

Figs. 3 and 4 show the variation of the first three-order dimensionless complex frequencies of the viscoelastic plate with dimensionless follower force q for the same dimensionless delay time $H = 10^{-5}$ and different aspect ratios $\lambda = 1.5$ and 2, respectively. In contrast with Fig. 2, in the case of $q = 0$, the first three natural frequencies of the viscoelastic plate increase with the increase of aspect ratio. And with the increase of q, the first and second divergence loads increase too.

Figs. 5–7 show the variation of the first three dimensionless complex frequencies of the viscoelastic plate with dimensionless follower force q for the dimensionless delay time $H = 10^{-3}$, and different aspect ratios

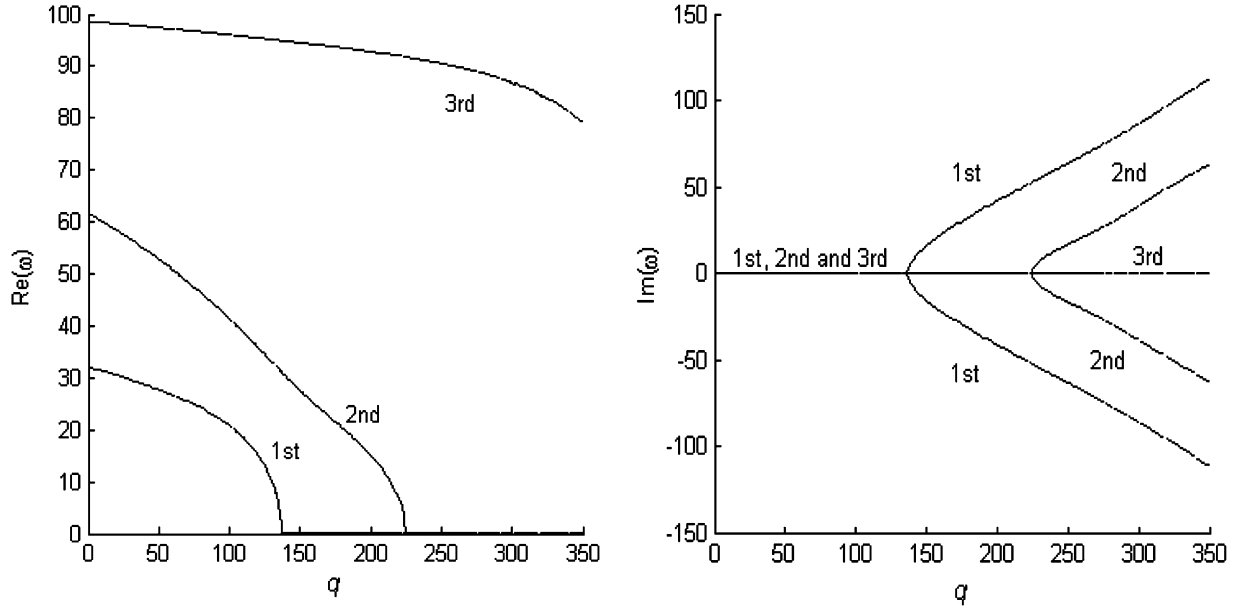

Fig. 3. The first three dimensionless complex frequencies ω vs. dimensionless follower force q for SSSS plate for $H = 10^{-5}$, $\lambda = 1.5$.

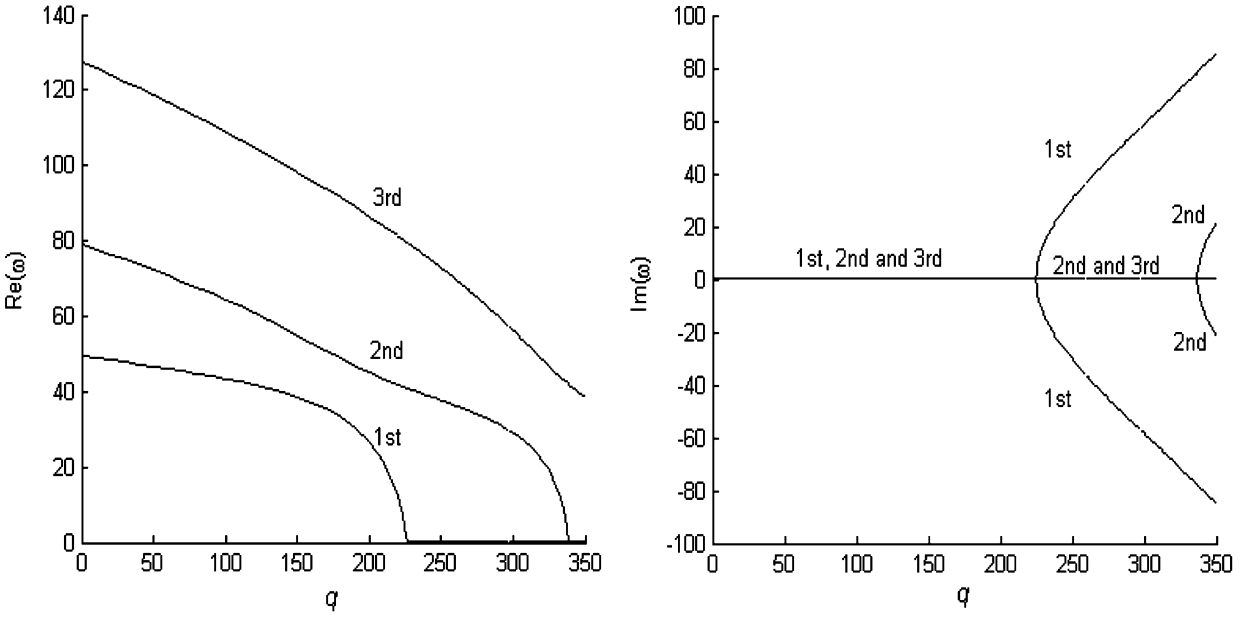

Fig. 4. The first three dimensionless complex frequencies ω vs. dimensionless follower force q for SSSS plate for $H = 10^{-5}$, $\lambda = 2$.

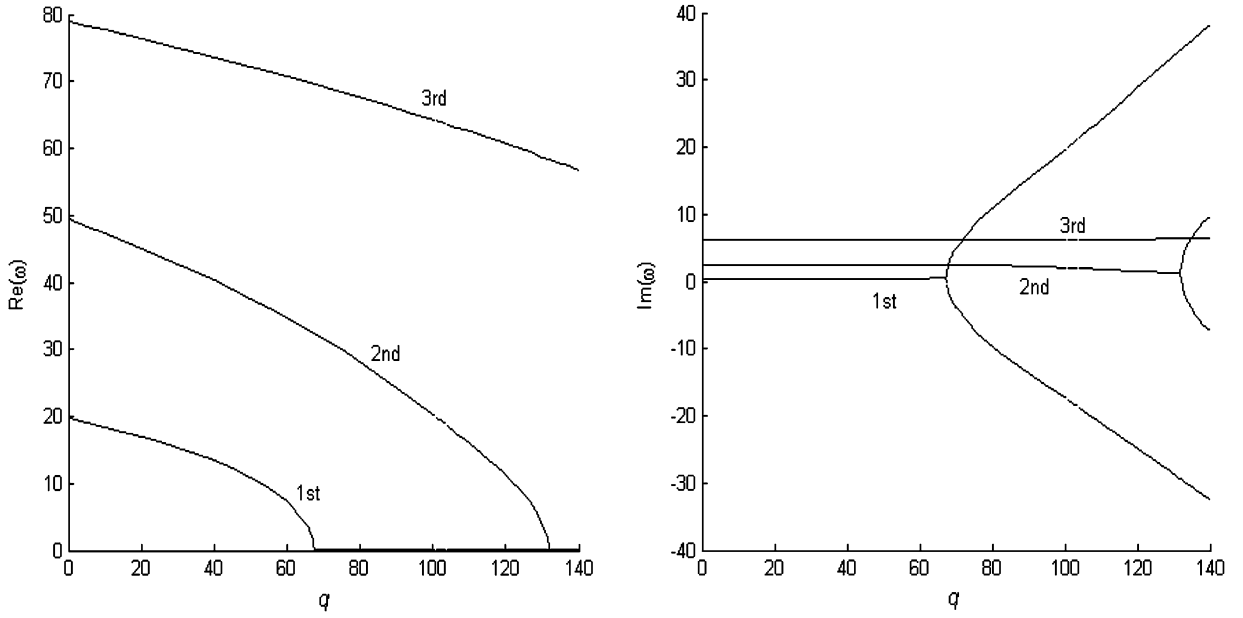

Fig. 5. The first three dimensionless complex frequencies vs. dimensionless follower force q for SSSS plate for $H = 10^{-3}$, $\lambda = 1$.

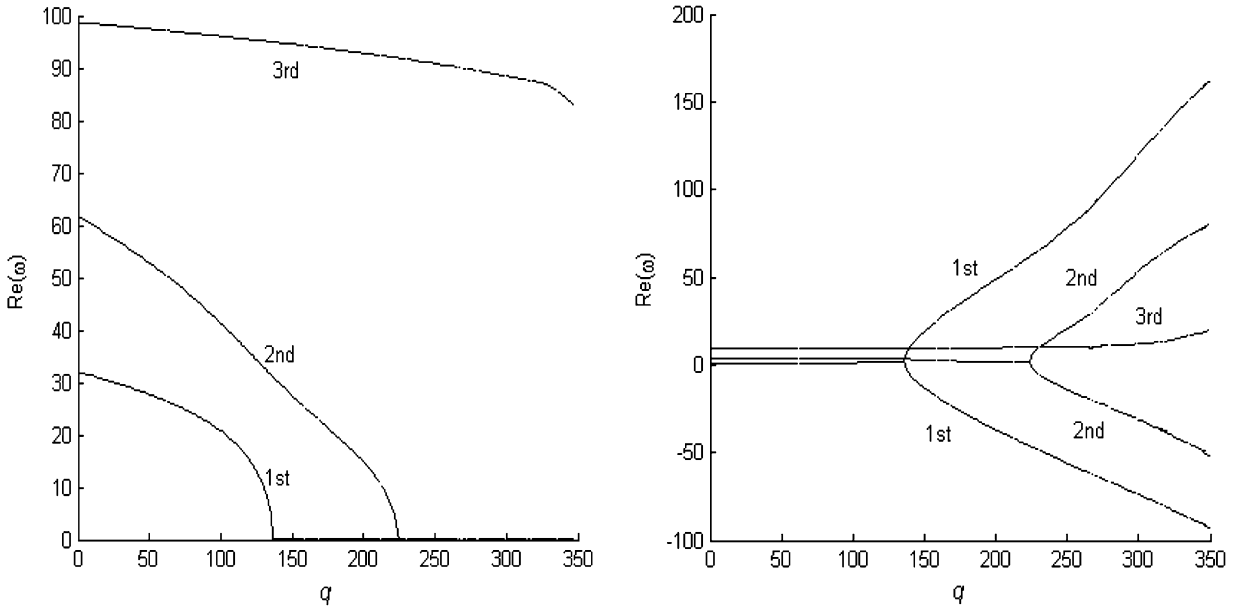

Fig. 6. The first three dimensionless complex frequencies vs. dimensionless follower force q for SSSS plate for $H = 10^{-3}$, $\lambda = 1.5$.

$\lambda = 1$, 1.5 and 2, respectively. In comparison with Figs. 2–4, respectively, it indicates that when $q = 0$, the first three natural frequencies of the viscoelastic plate decrease slightly because of the increase of dimensionless delay time H, the first and the second divergence loads decrease slightly with the increase of dimensionless delay time, the imaginary parts of the first three dimensionless complex frequencies do not remain zero but are positive values, and increase with the increase of the mode order at small dimensionless follower force.

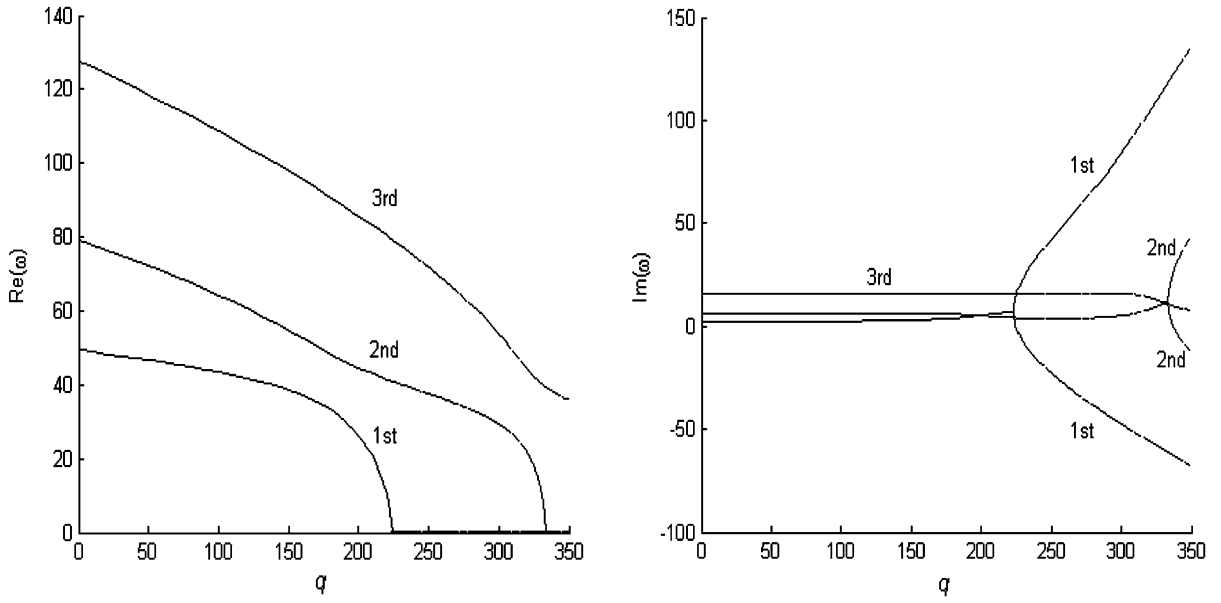

Fig. 7. The first three dimensionless complex frequencies vs. dimensionless follower force q for SSSS plate for $H = 10^{-3}$, $\lambda = 2$.

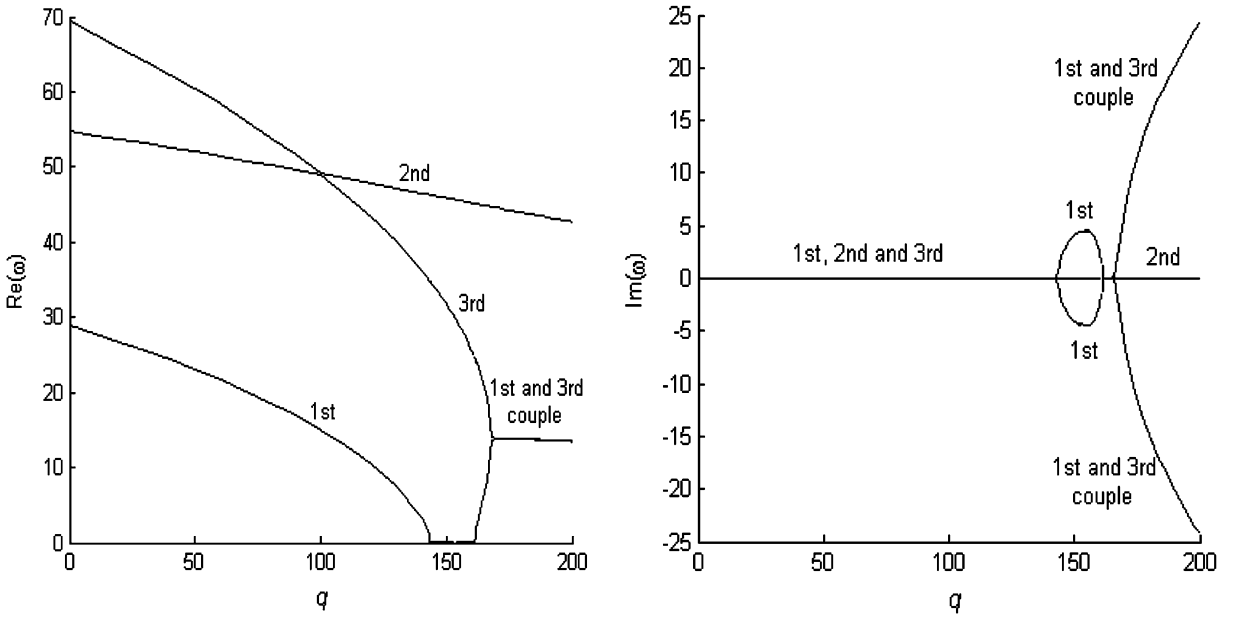

Fig. 8. The first three dimensionless complex frequencies vs. dimensionless follower force q for CSCS plate for $H = 10^{-5}$, $\lambda = 1$.

4.2. The plate with two opposite edges simply supported and other two edges clamped

Fig. 8 gives the variation of the first three dimensionless complex frequencies of the viscoelastic plate with dimensionless follower force q for $H = 10^{-5}$, $\lambda = 1$. As can be seen in Fig. 8, with the increase of q, the real part of ω decreases, while its imaginary part remains zero. When $q = 143.5$, the real parts of ω in the first-order mode become zero; subsequently, $\mathrm{Re}(\omega) = 0$, but $\mathrm{Im}(\omega) > 0$ and $\mathrm{Im}(\omega) < 0$. This indicates that the plate shows divergence instability in the first-order mode; $q_{d1} = 143.5$ is the first-order divergence load. With further

increase of q, the first and third mode frequency curves merge together, the two frequencies become complex conjugate and it forms a flutter-type instability. The load and frequency at which the plate undergoes coupled-mode flutter are termed as the flutter load and flutter frequency, respectively, that is to say the flutter load is $q_f = 168.00$.

Figs. 9 and 10 give the variation of the first three-order dimensionless complex frequencies of the viscoelastic plate with dimensionless follower force q for the dimensionless delay time $H = 10^{-5}$, and with different aspect

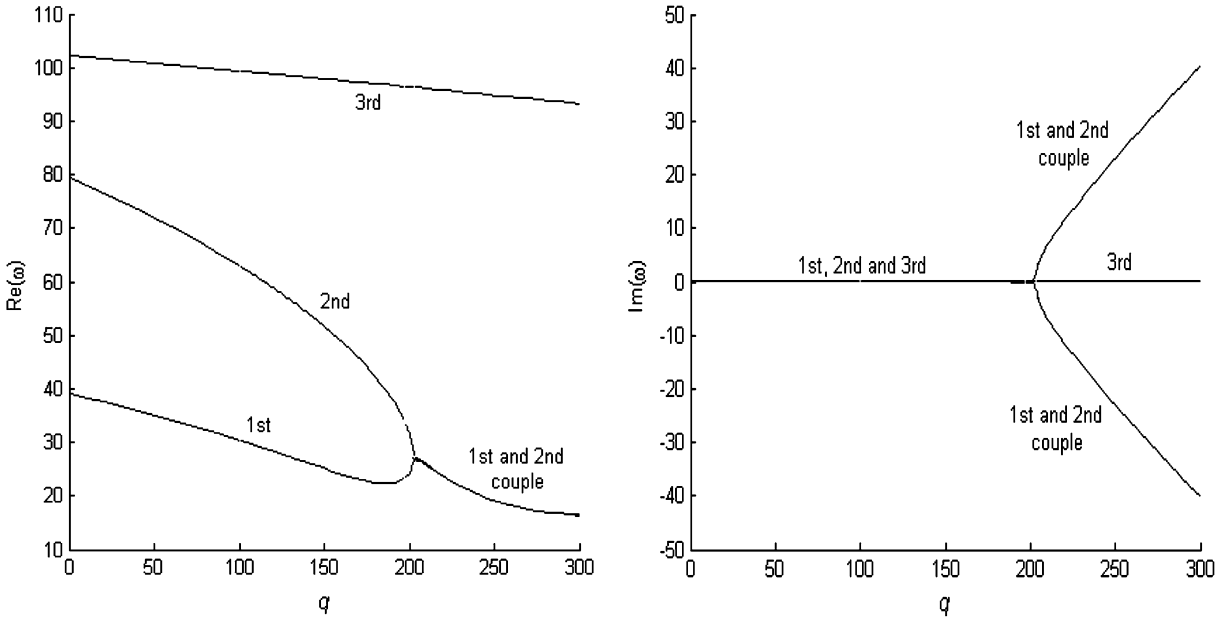

Fig. 9. The first three dimensionless complex frequencies vs. dimensionless follower force q for CSCS plate for $H = 10^{-5}$, $\lambda = 1.5$.

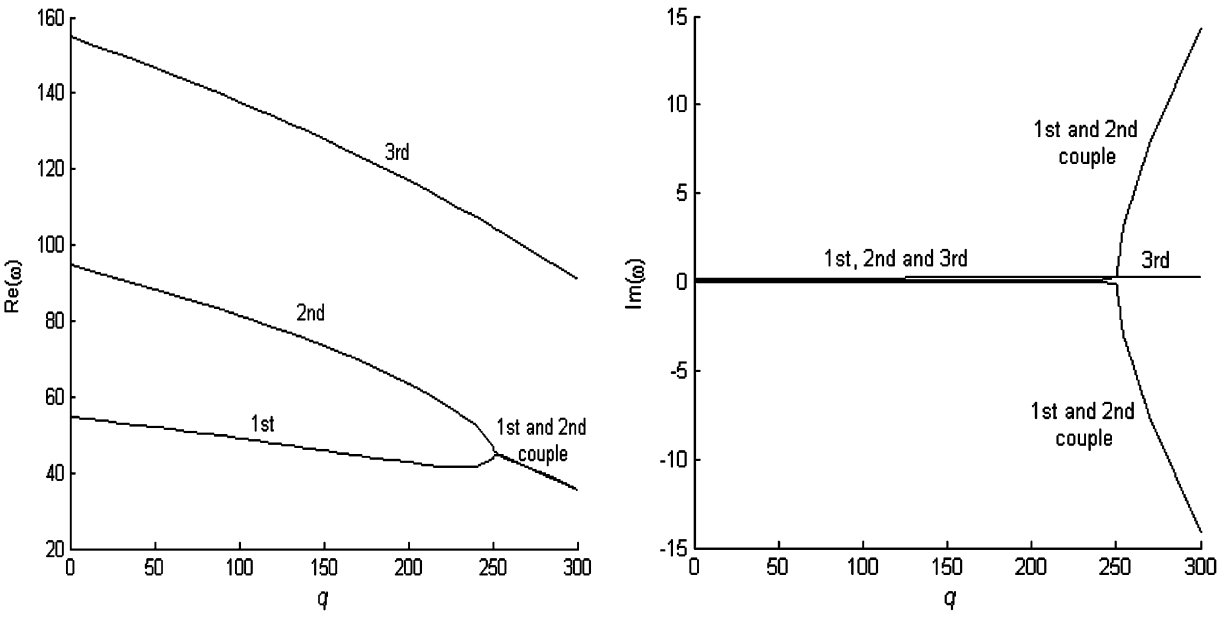

Fig. 10. The first three dimensionless complex frequencies vs. dimensionless follower force q for CSCS plate for $H = 10^{-5}$, $\lambda = 2$.

ratios $\lambda = 1.5$ and 2, respectively. In comparison with Fig. 8, it shows that the first three-order natural frequencies of the plate increase with the increase of aspect ratio, and with the increase of λ, the plate does not show divergence instability, it only undergoes flutter instability, and the modes in which the plate undergoes coupled-mode flutter is different from $\lambda = 1$.

Fig. 11 gives the variation of the first three-order dimensionless complex frequencies of the viscoelastic plate with dimensionless follower force q for $H = 10^{-3}$, $\lambda = 1$. In comparison with Fig. 8, it shows that when $q = 0$,

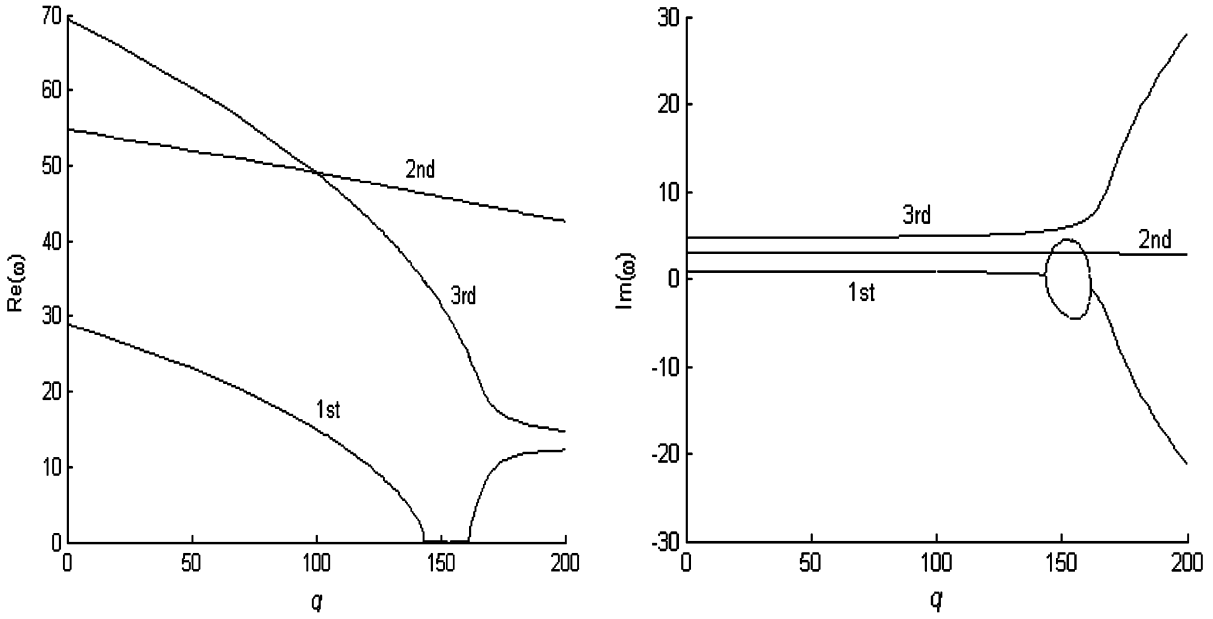

Fig. 11. The first three dimensionless complex frequencies vs. dimensionless follower force q for CSCS plate for $H = 10^{-3}$, $\lambda = 1$.

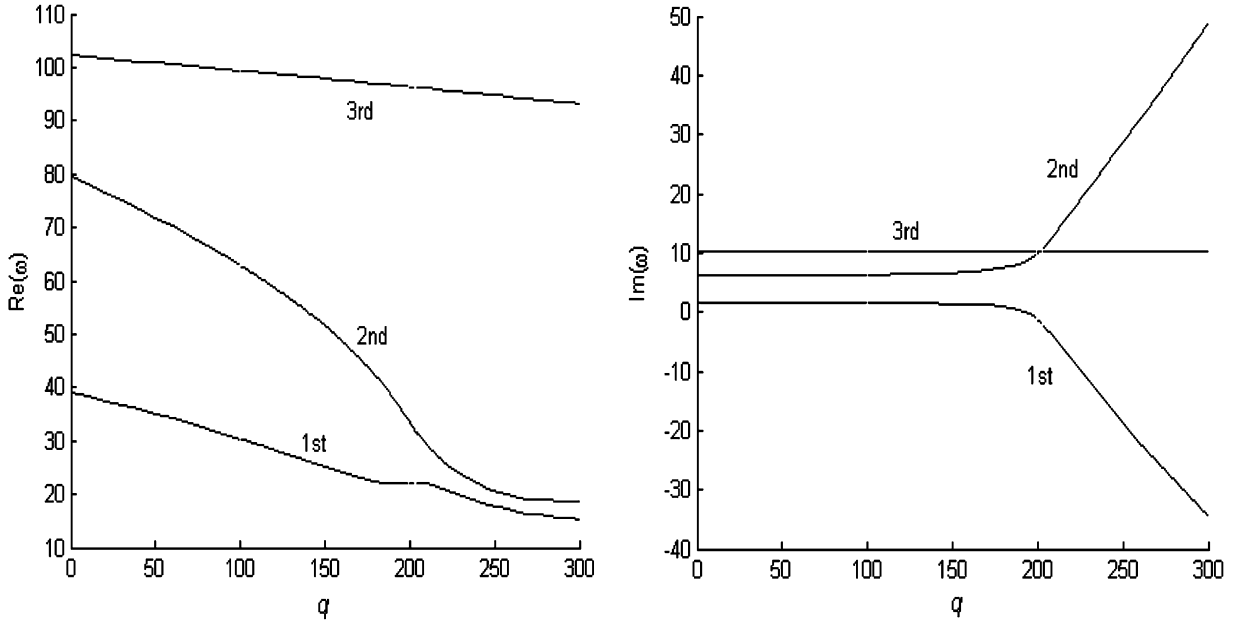

Fig. 12. The first three order dimensionless complex frequencies vs. dimensionless follower force q for CSCS plate for $H = 10^{-3}$, $\lambda = 1.5$.

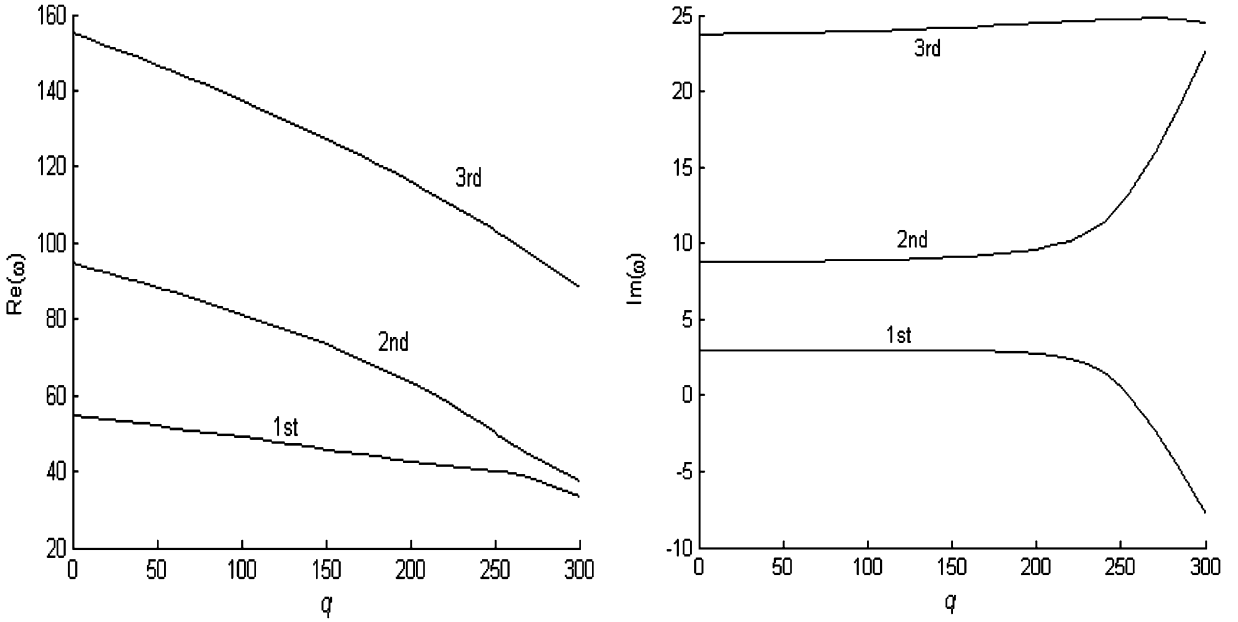

Fig. 13. The first three order dimensionless complex frequencies vs. dimensionless follower force q for CSCS plate for $H = 10^{-3}$, $\lambda = 2$.

the first three-order natural frequencies of the viscoelastic plate decrease slightly because of the increase of H. The plate exhibits a coupled-mode flutter, shows divergence instability in the first-order mode, and then undergoes single-mode flutter in the first-order mode. The imaginary parts of the first three-order mode dimensionless complex frequencies remain as positive values and not zero, and increase with the increase of the mode order at small dimensionless follower force.

Figs. 12 and 13 give the variation of the first three dimensionless complex frequencies of the viscoelastic plate with dimensionless follower force q for the same dimensionless delay time $H = 10^{-3}$, and with different aspect ratios $\lambda = 1.5$ and 2, respectively. In comparison with Figs. 9 and 10, respectively, it is observed that when $q = 0$, the first three-order natural frequencies of the viscoelastic plate decrease slightly because of the increase of dimensionless delay time. The first and the second mode do not couple, i.e., the plate does not undergo flutter instability, but it undergoes single-mode flutter in the first-order mode.

5. Conclusions

This paper analyzes flutter and divergence instabilities of a viscoelastic rectangular plate constituted by the Kelvin–Voigt model subjected to uniformly distributed tangential follower force, and deduces that the instability type and critical load of the viscoelastic plate are dependent on dimensionless delay time H, aspect ratio λ and boundary condition. Results of the analysis of the present study can be summarized as follows:

(1) In the case of dimensionless delay time $H \leqslant 10^{-5}$, the frequency and critical load of the non-conservative viscoelastic plate constituted by the Kelvin–Voigt model are close to those of the non-conservative elastic plate.
(2) For the viscoelastic plate with four edges simply supported, the general instability type is divergence instability, the corresponding critical load is divergence load. When the dimensionless delay time H is invariable, with the increase of the aspect ratio λ, the first three natural frequencies of the viscoelastic plate increase in the case of $q = 0$, the first and the second divergence loads increase too. While the aspect ratio λ keeps constant, with the increase of dimensionless delay time H, the first three natural frequencies decrease slightly in the case of $q = 0$, and the first and the second divergence loads also decrease slightly, the imaginary parts of the complex frequencies of the first three-order mode do not remain zero but are positive values, and increase with the increase of mode orders.

(3) For the viscoelastic plate with two opposite edges simply supported and other two edges clamped, the aspect ratio λ has great effect on the instability type of the plate. When $\lambda = 1$, the plate undergoes divergence instability first, then the plate shows flutter instability, in the case of $\lambda = 1.5$ and 2, the plate only undergoes flutter instability. When the dimensionless time H keeps constant, with the increase of the aspect ratio λ, the first three natural frequencies of the plate increase, and the divergence load or the flutter load increases too. When the aspect ratio λ keeps constant, with the increase of dimensionless delay time H, the first three natural frequencies decrease slightly, and the plate does not undergo flutter instability. Usually, the plate shows divergence instability in the first mode, then undergoes single-mode flutter in the first mode in the case of $\lambda = 1$, when $\lambda = 1.5$ and 2, the plate only does single-mode flutter in the first mode. At the same time, the imaginary parts of the complex frequencies of the first three modes remain positive values at small q, and increase with the increase of the mode orders.

Acknowledgements

The research was supported by the Foundation of Excellent Doctoral Dissertations of Xi'an University of Technology.

References

[1] S. Adali, Stability of a rectangular plate under non-conservative and conservative forces, *International Journal of Solids and Structure* 18 (1982) 1043–1052.
[2] H.H. Leipholz, F. Pfendt, Application of extend equations of Galerkin to stability problems of rectangular plates with free edges and subjected to uniformly distributed follower forces, *Computer Methods in Applied Mechanics and Engineering* 37 (1983) 341–365.
[3] Z.M. Wang, Y.Z. Ji, The dynamic stability of rectangular plates under the action of tangential follower force, *Journal of Vibration Engineering* 5 (1) (1992) 78–83.
[4] Q.H. Zuo, H.L. Shreyer, Flutter and divergence instability of non-conservative beams and plates, *International Journal of Solids and Structures* 33 (9) (1996) 1355–1367.
[5] J.H. Kim, J.H. Park, On the dynamic stability of rectangular plates subjected to intermediate follower forces, *Journal of Sound and Vibration, Letter to the Editor* 209 (5) (1998) 882–888.
[6] J.H. Kim, H.S. Kim, A study on the dynamic stability of plate under follower force, *Computers and Structures* 74 (2000) 351–363.
[7] G. Jayaraman, A. Struthers, Divergence and flutter instability of elastic specially orthotropic plates subject to follower forces, *Journal of Sound and Vibration* 281 (2005) 357–373.
[8] T.T. Darabseh, J. Genin, Dynamic stability of viscoelastic columns loaded by a follower force, *Journal of Mechanical Engineering Science* 218 (10) (2004) 1091–1101.
[9] M.A. Langthjem, Y. Sugiyama, Dynamic stability of viscoelastic beam under follower forces, *Journal of Sound and Vibration* 238 (5) (2000) 809–851.
[10] R.H. Zhuo, S.Z. Fen, Dynamic stability of viscoelastic beam under follower force, *Engineering Mechanics* 22 (3) (2005) 26–30.
[11] W. Flügge, *Viscoelasticity[M]*, Springer, Berlin, 1975.
[12] T.Q. Yang, *Viscoelasticity Theory and Applications*, Science Press, Beijing, 2004.
[13] T.M. Teo, K.M. Liew, A differential quadrature procedure for three-dimensional buckling analysis of rectangular plates, *International Journal of Solids and Structures* 36 (1999) 1149–1168.
[14] Ö. Civalek, Application of differential quadrature (DQ) and harmonic differential quadrature (HDQ) for buckling analysis of thin isotropic plates and elastic columns, *Engineering Structures* 26 (2004) 171–186.
[15] A.S.J. Al-Saifl, Zh.Y. Zhu, Upwind local differential quadrature method for solving coupled viscous flow and heat transfer equations, *Applied Mathematics and Mechanics* 25 (10) (2004) 1034–1041.
[16] D.J. Gorman, *Free Vibration Analysis of Rectangular Plates*, Elsevier North-Holland, Inc., 1982.